

Properties of the density matrix from realistic calculations

Xiaodong Zhang¹ and D. A. Drabold^{1,2}

¹*Department of Physics and Astronomy, Ohio University, Athens, Ohio 45701-2979*

²*Trinity College, Cambridge, CB2 1TQ, United Kingdom*

(Received 31 October 2000; revised manuscript received 22 January 2001; published 30 May 2001)

We compute the single-particle density matrix in large (500-, 512-, and 1000-atom) models of fcc aluminum and crystalline (diamond) and amorphous silicon and carbon. We use an approximate density functional Hamiltonian in the local density approximation. The density matrix for fcc aluminum is found to closely approximate the results for jellium, and the crystalline and amorphous insulators exhibit exponential decay albeit with pronounced anisotropy. We compare the computed decays to existing predictions of the fall off of the density matrix in insulators and find that the “tight-binding” prediction of Kohn [W. Kohn, Phys. Rev. **115**, 809 (1959)] provides the best overall fit to our calculations for Si and C.

DOI: 10.1103/PhysRevB.63.233109

PACS number(s): 71.55.Jv, 71.10.Ca, 71.15.Nc

I. INTRODUCTION

There is a continuing effort to improve the efficiency of single-electron methods for modeling materials. Examples of these are density functional approaches, and also simple but efficient tight-binding schemes. A unifying feature of these efforts is the need for a real-space localized representation for the one-electron states (Kohn-Sham orbitals in a density functional computation), or almost equivalently a real-space localized density matrix (DM). While there have been many calculations exploiting a real-space local representation,^{1,2} there have been few serious attempts to study the spatial decay of the DM in real materials and with realistic Hamiltonians (for linear alkanes, however, see Ref. 3). The DM is expected to provide a lower bound on how well localized the Wannier states may be (a useful explicit recipe for building these states to minimize their extent has recently been given⁴). In this paper, we directly compute the DM for a metal (Al) and for crystalline and amorphous phases of Si and C. Among other things, we show that Al is very free-electron-like, discuss the significant anisotropies in the DM in insulators, and compare the computed spatial decay to available predictions.

The single-particle density operator $\hat{\rho} = \{\exp[\beta(\hat{H} - \mu) + 1]\}^{-1}$ probes the spatial locality of electrons, and enables a spatially local formulation of the electronic structure problem (β is the inverse temperature and μ is the chemical potential). Kohn⁵ has stated this clearly. He called the dependence of ground state properties on the local environment “the principle of nearsightedness,” and observed that it “is generally a consequence of wave-mechanical destructive interference.” It is difficult to perform analytical calculations of $\rho(\mathbf{x}, \mathbf{x}') = \langle \mathbf{x} | \hat{\rho} | \mathbf{x}' \rangle$ in any but the simplest cases. As such, it is convenient to provide empirical insight from relatively realistic computations.

Li, Nunes, and Vanderbilt⁶ and Daw⁷ recognized that using a truncated $\rho(\mathbf{x}, \mathbf{x}')$ could lead to a linear scaling total energy and force method. In an atom-centered local representation $|\mu\rangle$, the band energy (for example) is just E_{bs}

$= \text{Tr}(\hat{\rho}\hat{H}) = \sum_{\nu} \sum_{\mu} \rho_{\nu\mu} H_{\mu\nu} \equiv \sum_{\nu} \Gamma_{\nu}$. Here, the sum index μ_{ν} emphasizes that only a finite number of terms (independent of system size and only from the local environment of basis functions near the site associated with ν) needs to be computed. Then the CPU time for computing E_{bs} scales as $N\tau_{\Gamma}$; the desired linear scaling, if τ_{Γ} is the average time to compute the “local” band energy for the “ ν locale” Γ_{ν} . For a detailed discussion, see the reviews of Goedecker⁸ and Ordejón.⁹

II. ELEMENTARY ESTIMATES OF THE DENSITY MATRIX

For the free electron gas at zero temperature, the DM is given in standard textbooks,¹⁰

$$\begin{aligned} \rho(\mathbf{x}, \mathbf{x}') &= 2(2\pi)^{-3} \int_{\mathbf{k} < \mathbf{k}_F} d^3k e^{-i\mathbf{k}\cdot(\mathbf{x}-\mathbf{x}')} \\ &= 3n[\sin(\zeta) - \zeta \cos(\zeta)]/\zeta^3, \end{aligned} \quad (1)$$

where $\zeta = k_F|\mathbf{x}-\mathbf{x}'|$, k_F is the Fermi wave vector, and n is the density of the electron gas.

The DM for this system has long range at $T=0$; the DM (and electron pair distribution function) wiggles and decays as a power law for $\zeta \rightarrow \infty$.¹⁰ The analytic origin of the slow decay is the abrupt cutoff at the Fermi surface, and is mathematically nothing more than a case of “Gibbs’ phenomenon,”¹¹ as seen in the theory of Fourier series. Of course it is quite physical in this case and is similar in origin to Friedel oscillations and the oscillatory Ruderman-Kittel-Kasuya-Yosida interaction. For finite temperature the decay envelope is exponential because of the smooth cutoff of the Fermi function.

The real-space DM shows an exponential decay behavior at zero temperature for insulators:¹²

$$\rho(\mathbf{x}, \mathbf{x}') \propto \exp(-\gamma|\mathbf{x}-\mathbf{x}'|). \quad (2)$$

Kohn¹³ proved the exponential decay behavior in the case of a one-dimensional model crystal. Stephan *et al.*¹⁴ observed that the exponential decay of orthogonalized Wannier func-

tions in crystalline and amorphous systems with similar local topological order (and a similar mobility gap) appears to be close.

Some simple predictions for the asymptotic decay of the DM are available. Ismail-Beigi and Arias¹⁵ predicted that for insulators in the weak binding limit one should observe an exponential decay with rate

$$\gamma_{wb} = aE_{gap}m/\hbar^2, \quad (3)$$

whereas Kohn¹³ suggested that in the tight-binding limit

$$\gamma_{tb} = (2E_{gap}m/\hbar^2)^{1/2}. \quad (4)$$

We compare these to our numerical calculations below. Units for all decay rates are \AA^{-1} .

III. CALCULATIONS

In this paper we implement reasonably realistic calculations, with an approximate density functional Hamiltonian due to Sankey and Niklewski.¹⁶ This Hamiltonian has four basis functions (pseudoatomic orbitals) per atom and employs the Harris functional and nonlocal pseudopotentials. The basis is nonorthogonal and the method has been well tested for the systems we describe here. We compute the DM as

$$\rho(\mathbf{x}, \mathbf{x}') = 2 \sum_{n \text{ occ}} \psi_n^*(\mathbf{x}) \psi_n(\mathbf{x}') \quad (5)$$

in which $\psi_n(\mathbf{x})$ is the n th eigenvector of the Sankey Hamiltonian. All calculations reported here were performed using exact diagonalization on 500-atom (Al) and 512-atom (Si,C) cells. As well as crystal phases, we use realistic models of a -Si and amorphous diamond (a -D) due to Djordjevic, Thorpe, and Wooten.¹⁷ Calculations are restricted to the Γ point of the Brillouin zone: the models are large enough to avoid \mathbf{k} sums in addition to the band sums. Occupations are computed for $T=0$. The DM's reported in this paper always adopt the midpoint between two atoms as origin. While not especially significant in metals, this is of course the bond center in the tetrahedral insulators we discuss later.

A. Metals

Equation (1) is derived from the free electron gas. It is not clear to what extent the electrons in a real metal mimic the free electron gas. To study the decay properties in a real metal, we extract the DM for a 500-atom model of fcc Al (the supercell is 20.25 \AA on a side). The DM is calculated from Eq. (5). Figure 1 gives the decay of the DM in this metal. Clearly, the electrons behave much like free particles in view of the near coincidence of the analytic result and the calculation from Eq. (5). The electron density used for Eq. (1) is $n = 0.185 \text{ \AA}^{-3}$ (the actual density of valence electrons) which leads to the Fermi vector $k_F = 1.763 \text{ \AA}^{-1}$.

To check the origin of the ringing in Fig. 1, we also considered a heavily p -doped insulator (c -Si) (by shifting the

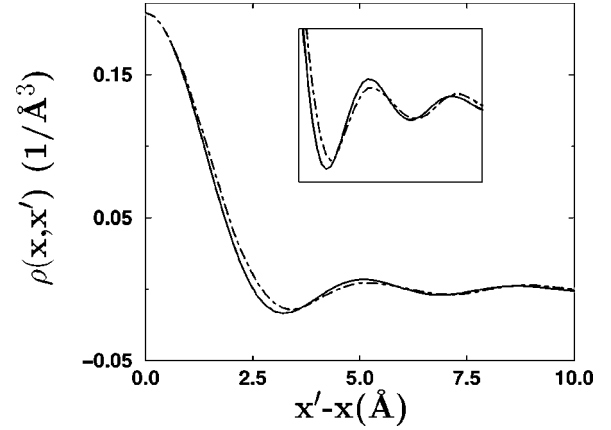


FIG. 1. The real-space density matrix for the 500-atom Al system. The inset is an enlargement of the density matrix for the tail region to show the oscillatory behavior. The dot-dashed line represents the calculation and the solid line is from Eq. (1).

Fermi level well into the valence states), and a power-law decay and ringing was observed as for Al.

B. Insulators

We have seen that the DM for Al is quite isotropic due to the delocalization of the valence electrons. For Si and C, we calculate the DM along several directions including parallel and orthogonal to the bond direction. As we show in Fig. 2, there is a large degree of anisotropy in the decay of the DM for a 1000-atom model of (a) diamond Si and (b) amorphous Si. The decay appears to be most rapid and monotonic along directions significantly different from the bond direction or the direction orthogonal to it. The decay is slowest in the longitudinal (bond parallel) direction. This result is in qualitative agreement with results for orthonormal Wannier func-

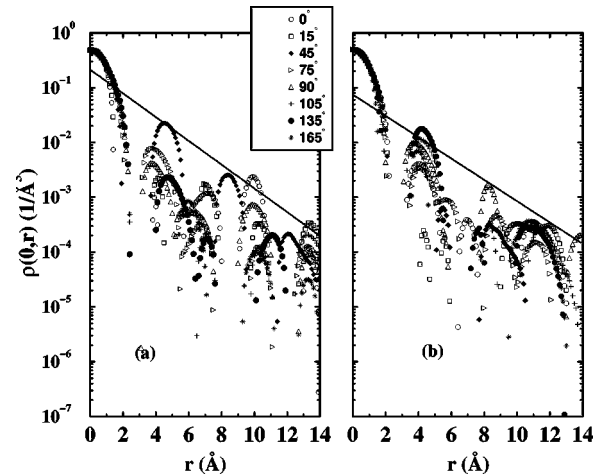


FIG. 2. Real-space density matrix for 1000-atom model of (a) diamond Si and (b) amorphous Si, both plotted on a logarithmic scale. The curves indicate the decay of the density matrix for different directions from the bond center. Here 0° refers to the bond direction, 90° is orthogonal to the bond, etc. The lines plotted are intended to be representative of the overall decay, and have slope $\gamma = 0.49 \text{ \AA}^{-1}$ for the crystal and $\gamma = 0.45 \text{ \AA}^{-1}$ for amorphous Si.

tions reported in Ref. 14. The box size for the 1000-atom *c*-Si model is 27.15 Å and for *a*-Si 27.694 Å.

We have checked the formula of Ref. 15. Using experimental values for a and E_g , the authors obtain $\gamma_{wb} \approx 0.8 \text{ \AA}^{-1}$ and 2.5 \AA^{-1} for *c*-Si and *c*-C, respectively. Kohn's prediction¹³ for the tight-binding regime [Eq. (4)] yields $\gamma_{tb} \approx 0.54 \text{ \AA}^{-1}$ for Si and $\gamma_{tb} \approx 1.19 \text{ \AA}^{-1}$ for C. Evidently these two approaches give reasonably similar results for Si, but very different rates for C. Best fits from our calculations give $\gamma \approx 0.49 \text{ \AA}^{-1}$ for *c*-Si and $\gamma \approx 1.34 \text{ \AA}^{-1}$ for *c*-C, in rather good agreement with the estimate of Kohn for both materials and in reasonable agreement with Ismail-Beigi and Arias¹⁵ for Si. In fairness to the authors of Ref. 15, they would not expect C to be well described by their expression [Eq. (3)]. We should note that there is such an important effect from directional anisotropy that there is some significant uncertainty (of order 0.05 \AA^{-1} in the decays reported). The rates reported here are from a calculation on a 1000-atom model of *c*-Si and a 512-atom model of diamond (box size 14.24 Å).

Next, we discuss the DM for a 1000-atom model of amorphous Si (Ref. 18) and a 512-atom model of *a*-diamond.¹⁷ These disordered networks have much of the local (tetrahedral) character of diamond albeit without long range order. We observe that the asymptotic decay rates for *c*-Si and *a*-Si are not very different. Stephan *et al.*¹⁴ conjectured that the decay of the Wannier functions WF's (as well of the as DM's) is related to separation of the extended occupied and unoccupied states (similar for these amorphous and crystalline models), i.e., the width of the mobility gap, a statement consistent with our work. While there is minor variation in decay rates, within fitting uncertainty, all decay rates for *a*-Si are similar (and approximately equal to the result for the crystal), independent of whether a strained bond or a "typical" bond is selected, within the uncertainty due to anisotropy. The same is true for *a*-D. We emphasize that the short range character of the DM depends strongly on the choice of bond, but not the behavior of the tail of the DM. One can interpret this as a consequence of the work of Rehr and Kohn¹⁹ and of Kohn and Onffroy,²⁰ who show that long range decay of the DM is very similar for "ordinary" or highly defective sites. We observed a similar insensitivity in the tail when we introduced artificial defects in *c*-Si. We also observe that Stephan, Martin, and Drabold¹⁴ noted that orthogonalized Wannier functions for *a*-Si have an intricate nonspherical structure depending on the disorder in the material, which is consistent with our work.

In Fig. 3, we report contour plots for the DM starting at a bond center. The figure shows the DM's for the crystal [Fig. 3(a)], and two sites (tetrahedral and defective) for *a*-Si [Figs. 3(b) and 3(c)]. Notice that the DM shows a clear tendency to become nonspherical in all cases, reflecting the directionality of the covalent bond. In a disordered environment, this symmetry is retained near the origin for a normal (tetrahedral) environment and destroyed at larger correlation length [Fig. 3(b)]. In *a*-Si, even the structure near the origin for the non-tetrahedral environment is distorted, producing a rather ir-

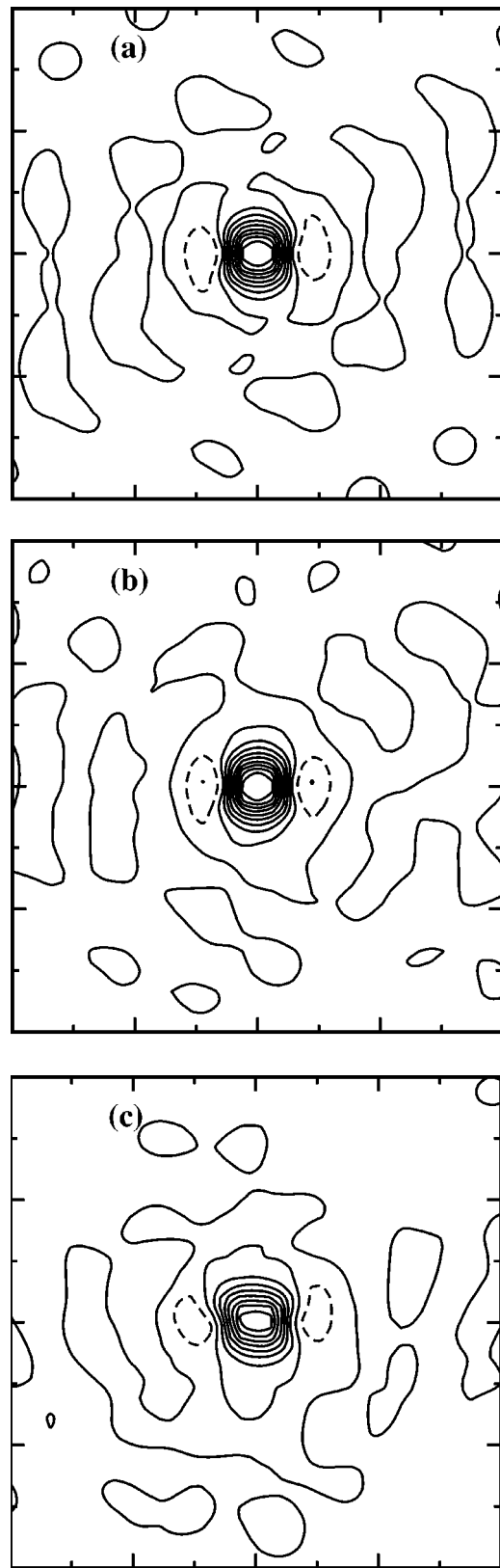


FIG. 3. Contour plot of real-space density matrix for (a) *c*-Si, (b) *a*-Si at tetrahedral bond, and (c) *a*-Si at a badly strained bond. The abscissa is the longitudinal and the ordinate the transverse direction relative to the bond. Box edge is 20 Å (these cells have 512 atoms). The dashed lines indicate regions for which the density matrix becomes negative.

regular structure in the whole space [Fig. 3(c)]. The anisotropy that we have discussed is made quite apparent in these figures.

IV. CONCLUSION

We have used a simplified *ab initio* Hamiltonian to investigate the decay of the density matrix in a metal and in crystalline and amorphous insulators. The DM for Al is found to be very close to the free electron prediction. For insulators,

there is a large anisotropy in the DM, with decay especially slow along the bond direction.

ACKNOWLEDGMENTS

This work was performed in part under the auspices of the U.S. NSF under Grant Nos. DMR-00-81006 and DMR-00-74624. We acknowledge helpful discussions with Dr. Uwe Stephan and Professor R. M. Martin. D.A.D. thanks Professor S. R. Elliott and Trinity College, Cambridge for financial support and their hospitality.

-
- ¹P. Ordejón, D.A. Drabold, R.M. Martin, and M.P. Grumbach, Phys. Rev. B **51**, 1456 (1995); **48**, 14 646 (1993).
- ²F. Mauri, G. Galli, and R. Car, Phys. Rev. B **47**, 9973 (1993).
- ³P.E. Maslen, C. Ochsensfeld, C.A. White, M.S. Lee, and M. Head-Gordon, J. Phys. Chem. A **102**, 2215 (1998).
- ⁴N. Marzari and D. Vanderbilt, Phys. Rev. B **56**, 12 847 (1997).
- ⁵W. Kohn, Phys. Rev. Lett. **76**, 3168 (1996).
- ⁶X.-P. Li, R.W. Nunes, and D. Vanderbilt, Phys. Rev. B **47**, 10 891 (1993).
- ⁷M.S. Daw, Phys. Rev. B **47**, 10 895 (1993).
- ⁸Stefan Goedecker, Rev. Mod. Phys. **71**, 1085 (1999).
- ⁹P. Ordejón, Comput. Mater. Sci. **12**, 157 (1998).
- ¹⁰Gordon Baym, *Lectures on Quantum Mechanics* (Benjamin/Cummings, New York, 1969), p. 424.
- ¹¹J.W. Gibbs, Nature (London) **59**, 200 (1898); **59**, 606 (1899); quoted in R. Courant and D. Hilbert, *Methods of Mathematical Physics* (Wiley Interscience, New York, 1953), Vol. 1, p. 105.
- ¹²J. des Cloizeaux, Phys. Rev. **135**, A685 (1964); **135**, A698 (1964).
- ¹³W. Kohn, Phys. Rev. **115**, 809 (1959); Chem. Phys. Lett. **208**, 167 (1993).
- ¹⁴U. Stephan, R.M. Martin, and D.A. Drabold, Phys. Rev. B **62**, 6885 (2000); U. Stephan and D.A. Drabold, *ibid.* **57**, 6391 (1998).
- ¹⁵S. Ismail-Beigi and T. Arias, Phys. Rev. Lett. **82**, 2127 (1999).
- ¹⁶O.F. Sankey and D.J. Niklewski, Phys. Rev. B **40**, 3979 (1989).
- ¹⁷B.R. Djordjevic, M.F. Thorpe, and F. Wooten, Phys. Rev. B **52**, 5685 (1995).
- ¹⁸G.T. Barkema and N. Mousseau, Phys. Rev. B **62**, 4985 (2000); For electron states and localization, see M. Durandurdu, D.A. Drabold, and N. Mousseau, *ibid.* **62**, 15 307 (2000).
- ¹⁹J.J. Rehr and W. Kohn, Phys. Rev. B **10**, 448 (1974).
- ²⁰W. Kohn and J.R. Onffroy, Phys. Rev. B **8**, 2495 (1973).